

Supporting Information

Enhanced driving force and charge separation efficiency of protonated anthraquinone for C-H photooxygenation of alkane by proton-coupled electron transfer

Hui Yin, Yingying Yuan, Yangbin Li, Jing Tang, Wenzhou Zhong and Liqiu Mao**

National & Local United Engineering Laboratory for New Petrochemical Materials & Fine Utilization of Resources, Key Laboratory of Chemical Biology Traditional Chinese Medicine Reserach Ministry of Education, College of Chemistry and Chemical Engineering, Hunan Normal University, Changsha 410081, P. R.

Table of Contents

I. Effects of different photocatalytic reaction conditions	S2
II. Comparison of the results of cyclohexane photooxidation and references	S3
III. Self-assembly photo-reactor used in this study	S5
IV. Effect of HCl/ethylAQs on photocatalytic reaction	S6
V. UV-Vis spectra of the samples	S7
VI. Cyclic voltammograms (CVs) of the samples.	S8
VII. Electronic properties of AQ and 2-ethylAQ-H₃PO₄	S9
VIII. Calculated UV-Vis spectra of 2-ethylAQ in different solvents	S10

Table S1 Effects of different solvents on the photocatalytic reactions

Entry	Solvent	Conv. (%)	Sele. (%)		
1	Acetonitrile	8.9	28.9	46.9	24.2
2	Ethanol	3.2	40.4	39.2	20.4
3	Acetone	36.2	18.9	80.2	0.8
4	Ethyl acetate	4.2	37.9	40.5	21.6
5	Benzene	10.7	12.6	52.6	34.8
6	Benzonitrile	8.2	81.3	9.9	8.8
7	Dichloromethane	7.6	66.2	0.5	33.3
8	DMF	0.8	38.3	15.3	46.4

Reaction conditions: 1.2 mmol cyclohexane, 0.1 mmol 2-ethylAQ photocatalyst, 5 mL solvent, 0.06 mL concentrated hydrochloric acid additive (0.7 mmol HCl), 35W tungsten–bromine lamp ($\lambda > 400$ nm), O₂ (0.1 MPa), at about 20 °C 24 h.

Table S2 Effects of the reaction times on the photocatalytic reactions

Entry	t (min)	Conv. (%)	Sele. (%)		
1	20	1.0	22.6	77.2	0.3
2	40	1.1	15.7	83.5	0.8
3	60	1.4	49.2	45.7	5.1
4	90	1.9	55.6	37.9	6.5
5	120	2.6	49.3	49.1	1.6

Reaction conditions: 1.2 mmol cyclohexane, 0.1 mmol 2-ethylAQ photocatalyst, 5 mL solvent, 0.06 mL concentrated hydrochloric acid additive (0.7 mmol HCl), 35W tungsten–bromine lamp ($\lambda > 400$ nm), O₂ (0.1 MPa), at about 20 °C.

Table S3 Comparison of the results of oxidation reaction of cyclohexane under different photooxidation systems

Entry	Catalyst	Oxidant/ (MPa)	T (°C)	t (h)	Solvent	Conv. (%)	KA-oil Sele. (%)	Ref.
1 ^{a, h}	5%-VOSO ₄ -HTS	O ₂ (0.1)	36,	6	MeCN	14.5	94.0	[1]
2 ^b	Fe _{0.2} Ti _{0.02} -SBA	O ₂ (0.25)	rt.	48	MeCN	2.3	>99	[2]
3 ^c	NH ₂ -M125/P25-4	O ₂ (0.1)	25	5	MeCN	0.7	99	[3]
4 ^c	N-TiO ₂ -3	O ₂ (0.1)	25	7	CCl ₄	0.1	100	[4]
5 ^d	WO ₃ NCs-AgNPs	TBHP	rt.	48	None	40.2	97.0	[5]
6 ^e	Cu-40min/a-C ₃ N ₄	H ₂ O ₂	60	4	MeCN	88.0	95	[6]
7 ^f	WO ₃ -NCDs	Air (1.5)	120	8	Acetone	7.9	98.9	[7]
8 ^f	MoO ₃ -Ag80	Air (1.5)	120	8	Acetone	8.6	99	[8]
9 ^{g, i}	BiOI	Air (0.1)	rt.	3	None	<0.1	98.8	[9]
10 ^{f, h}	VOCl ₂	O ₂ (0.1)	30	4	MeCN	23.3	97.0	[10]
11 ^{a, h}	V ^{IV} OQ ₂	O ₂ (0.1)	30	10	MeCN	18.7	86	[11]
12 ^{a, h}	2-EthylAQ	O ₂ (0.1)	rt.	24	Acetone	36.2	99.8	This work
13 ^{a, j}	2-EthylAQ	O ₂ (0.1)	rt.	10	Acetone	24.9	100	This work

^a 35 W bromine tungsten lamp; ^b solar simulator ($\lambda > 300$ nm, 1.5 AM); ^c 300 W Xenon lamp ($\lambda \geq 420$ nm); ^d 220 W Xenon lamp; ^e 400 W Xenon lamp ($\lambda \geq 420$ nm); ^f 300 W Xenon lamp; ^g 400 W metal halide lamp; ^h HCl as additive; ⁱ water as additive; ^j KH₂PO₄ as additive;

References

- [1] W. Zhong, T. Qiao, J. Dai, L. Mao, Q. Xu, G. Zou, X. Liu, D. Yin, and F. Zhao, Visible-light-responsive sulfated vanadium-doped TS-1 with hollow structure: Enhanced photocatalytic activity in selective oxidation of cyclohexane, *J. Catal.*, 2015, **330**, 208-221. <https://doi.org/10.1016/j.jcat.2015.06.013>.
- [2] Y. Ide, M. Iwata, Y. Yagenji, N. Tsunooji, M. Sohmiya, K. Komaguchi, T. Sano and Y. Sugahara, Fe oxide nanoparticles/Ti-modified mesoporous silica as a photo-catalyst for efficient and selective cyclohexane conversion with O₂ and solar light, *J. Mater. Chem. A*, 2016, **4**, 15829-15835. <https://doi.org/10.1039/c6ta04222h>.
- [3] X. Zhao, Y. Zhang, P. Wen, G. Xu, D. Ma and P. Qiu, NH₂-MIL-125(Ti)/TiO₂ composites as superior visible-light photocatalysts for selective oxidation of cyclohexane, *Mol. Catal.*, 2018, **452**, 175-183. <https://doi.org/10.1016/j.mcat.2018.04.004>.
- [4] G. Xu, Y. Zhang, D. Peng, D. Sheng, Y. Tian, D. Ma and Y. Zhang, Nitrogen-doped mixed-phase TiO₂ with controllable phase junction as superior visible-light photocatalyst for selective oxidation of cyclohexane, *Appl. Surf. Sci.*, 2021, **536**, 147953-147964, <https://doi.org/10.1016/j.apsusc.2020.147953>.
- [5] Y. Xiao, J. Liu, J. Mai, C. Pan, X. Cai and Y. Fang, High-performance silver nanoparticles coupled with monolayer hydrated tungsten oxide nanosheets: The structural effects in photocatalytic oxidation of cyclohexane, *J. Colloid. Interface Sci.*, 2018, **516**, 172-181. <https://doi.org/10.1016/j.jcis.2018.01.057>.
- [6] A. Shahzeydi, M. Ghiaci, H. Farrokhpour, A. Shahvar, M. Sun and M. Saraji, Facile and green synthesis of copper nanoparticles loaded on the amorphous carbon nitride for the oxidation of cyclohexane, *Chem. Eng. J.*, 2019, **370**, 1310-1321. <https://doi.org/10.1016/j.cej.2019.03.227>.

-
- [7] J. Zhang, J. Liu, X. Wang, J. Mai, W. Zhao, Z. Ding and Y. Fang, Construction of Z-scheme tungsten trioxide nanosheets-nitrogen-doped carbon dots composites for the enhanced photothermal synergistic catalytic oxidation of cyclohexane, *Appl. Catal. B Environ.*, 2019, **259**, 118063, <https://doi.org/10.1016/j.apcatb.2019.118063>.
 - [8] X. Wang, Z. Feng, J. Liu, Z. Huang, J. Zhang, J. Mai and Y. Fang, In-situ preparation of molybdenum trioxide-silver composites for the improved photothermal catalytic performance of cyclohexane oxidation, *J. Colloid Interface Sci.*, 2020, **580**, 377-388, <https://doi.org/10.1016/j.jcis.2020.07.015>.
 - [9] D. Contreras, V. Melin, K. Márquez, G. Pérez-González, H. D. Mansilla, G. Pecchi and A. Henríquez, Selective oxidation of cyclohexane to cyclohexanol by BiOI under visible light: Role of the ratio (1 1 0)/(0 0 1) facet, *Appl. Catal. B Environ.*, 2019, **251**, 17-24, <https://doi.org/10.1016/j.apcatb.2019.03.058>.
 - [10] Y. Wan, Q. Guo, K. Wang and X. Wang, Efficient and selective photocatalytic oxidation of cyclohexane using O₂ as oxidant in VOCl₂ solution and mechanism insight, *Chem. Eng. Sci.*, 2019, **203**, 163-172, <https://doi.org/10.1016/j.ces.2019.03.079>.
 - [11] J. She, X. Lin, Z. Fu, J. Li, S. Tang, M. Lei, X. Zhang, C. Zhang and D. Yin, HCl and O₂ co-activated bis(8-quinolinolato) oxovanadium (iv) complexes as efficient photoactive species for visible light-driven oxidation of cyclohexane to KA oil, *Catal. Sci. Tech.*, 2019, **9**, 275-285, <https://doi.org/10.1039/c8cy01241e>.



Figure S1 Photograph of the package box of lamp (which the instruction of lamp's package box clearly shows that the UV light has been filtered).

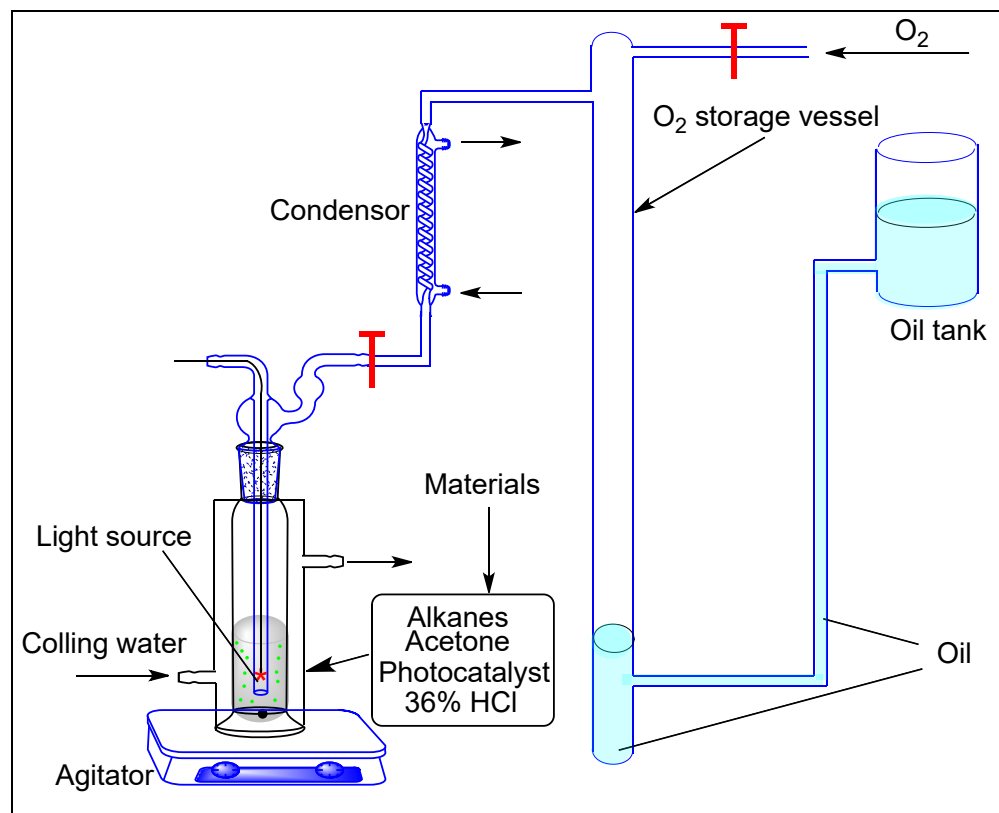


Figure S2 Self-assembly photo-reactor used in this study.

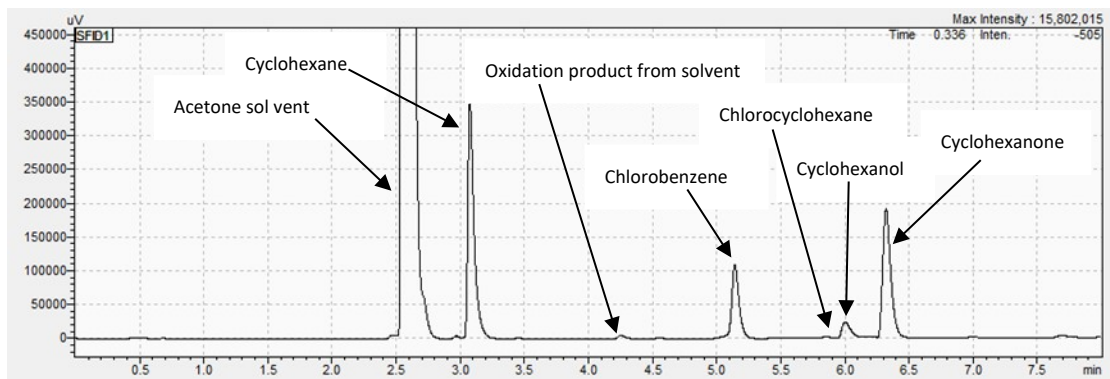


Figure S3 Gas chromatogram of product distribution

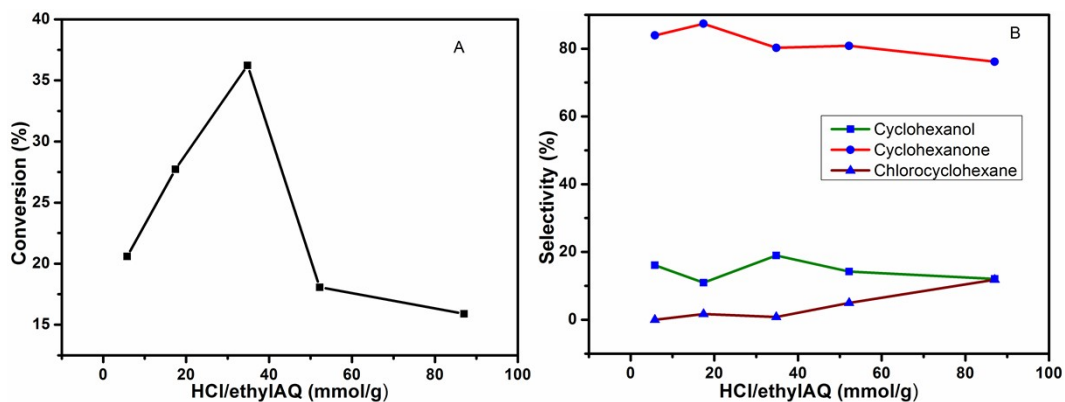


Figure S4 Effect of HCl/ethylAQs on photocatalytic reaction.

Reaction conditions: 1.2 mmol cyclohexane, 0.1 mmol 2-ethylAQ photocatalyst, 5mL acetone, 0.06 mL concentrated hydrochloric acid additive (0.7 mmol HCl), 35 W tungsten–bromine lamp ($\lambda > 400$ nm), O₂ (0.1 MPa), at about 20 °C. 24 h.

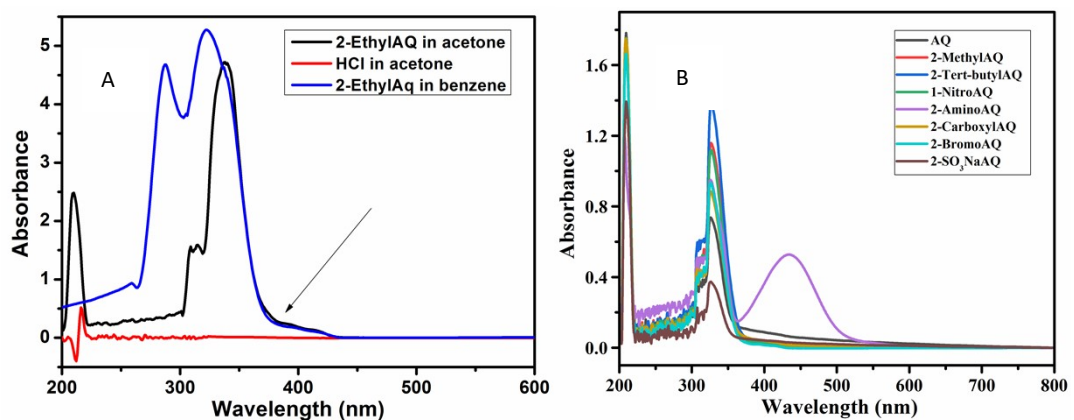


Figure S5 UV-Vis spectra of 2-ethylAQ or HCl (A) and other AQ derivatives (B).

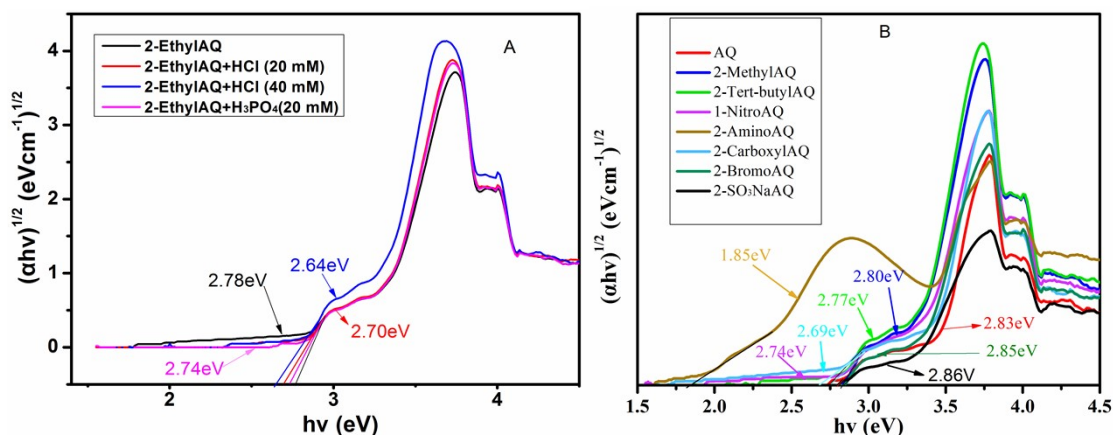


Figure S6 Tauc plots from UV-Vis spectra of 2-ethylAQ with acids (A) and other AQ derivatives (B).

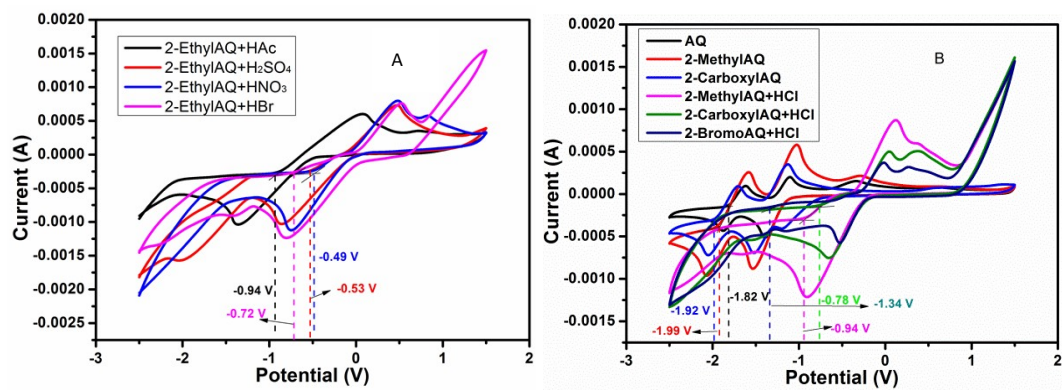


Figure S7 Cyclic voltammograms (CVs) of ethylAQ+acids (A) and other AQ derivatives (B) in acetone.

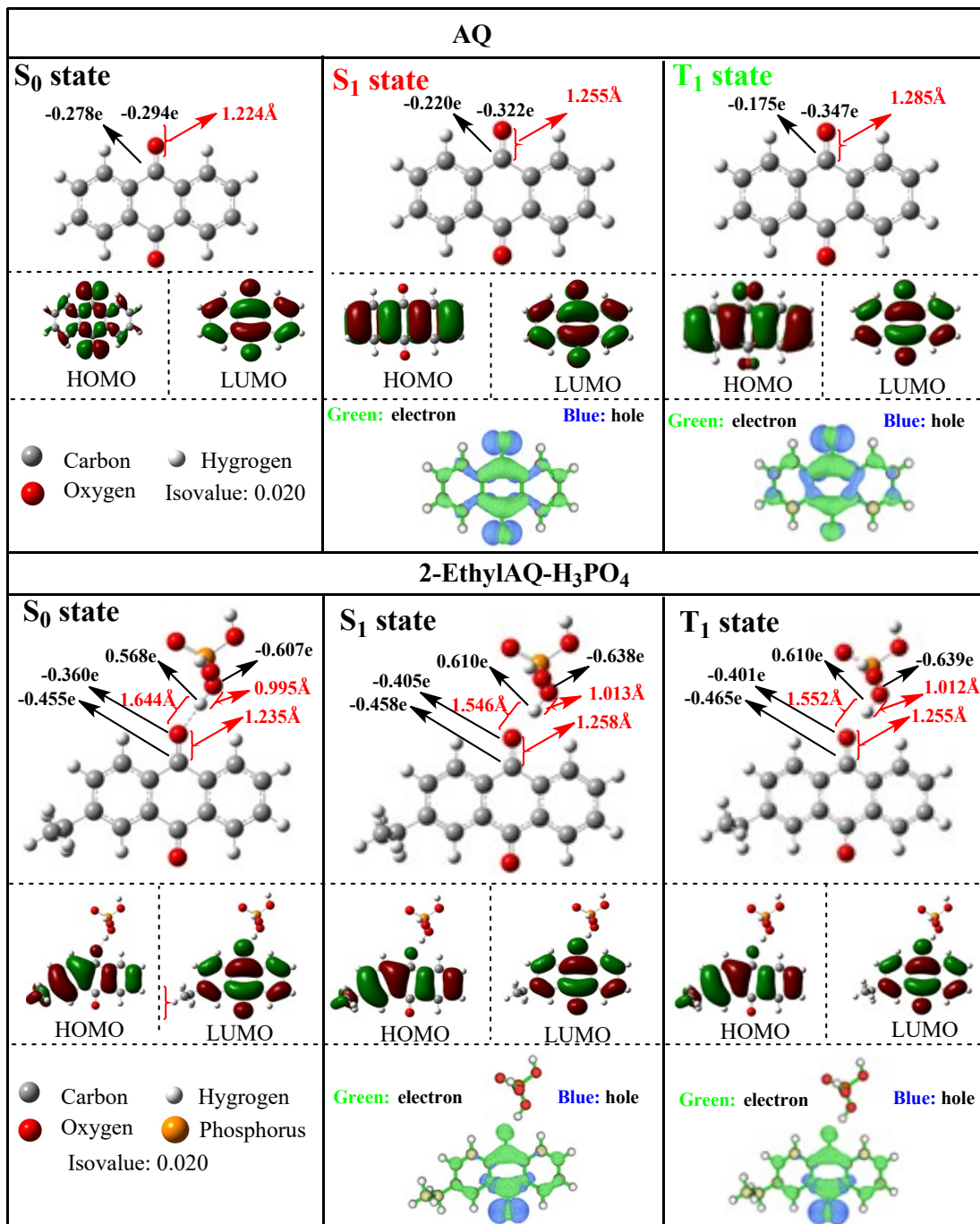


Figure S8 Electronic properties of optimized AQ and 2-ethylAQ-H₃PO₄ structures in the S₀, S₁ and T₁ states

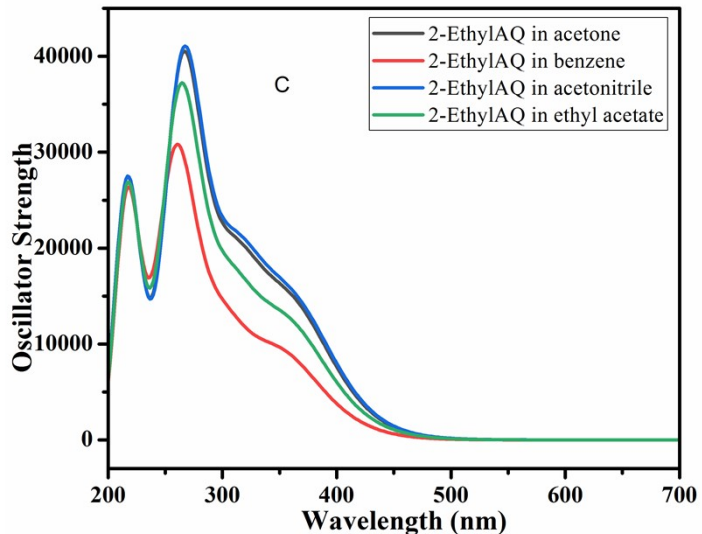


Figure S9 Calculated UV-Vis spectra of 2-ethylAQ in different solvents